Supplemental Information

Malectin - a novel carbohydrate-binding protein of the endoplasmic reticulum and a candidate player in the early steps of protein *N*-glycosylation

Thomas Schallus, Christine Jaeckh, Krisztina Féher, Angelina S. Palma, Yan Liu, Jeremy C. Simpson, Mukram Mackeen, Gunter Stier, Toby J. Gibson, Ten Feizi, Tomas Pieler, and Claudia Muhle-Goll

Supplemental Material and Methods

Sequence analysis of malectin and malectin-like proteins

In the *Xenopus laevis* malectin sequence UniProtKB/TrEMBL accession number Q6INX3 and the human homologue with gene name KIAA0152 and accession Q14165, the SMART server (Letunic et al., 2006) identified a signal peptide using the SignalP algorithm (Emanuelsson et al., 2007) and the transmembrane domain using TMHMM2 (Sonnhammer et al., 1998). Metazoan homologues were retrieved with NCBI Blast (hhtp://www.ncbi.nlm.nih.gov/BLAST/) searching the NR non-redundant database, then aligned with Clustal X (Chenna et al., 2003) and edited to tidy the gaps with SeaView (Galtier et al., 1996).

The homologous domain in plant RLKs was identified with NCBI PSI-BLAST searching the NR non-redundant database. The first iteration used the *X. laevis* malectin globular domain (residues 29-211). The second iteration was seeded with the set of metazoan sequences (all E-values < e-30). The third iteration included the ciliate malectin-like proteins and retrieved many plant receptor-like kinases (RLKs) with E-values spanning e-9 – e-5. Addition of any plant RLKs at all into a fourth iteration essentially collects a very large number of plant homologues generated by the genome projects (and is complicated by the fact that agricultural plants are polyploids). Reciprocal PSI-BLAST searches with the plant domain will retrieve the animal sequences, but the returned list becomes very large and unwieldy, due to all these plant sequences. Bacterial carbohydrate-binding proteins are retrieved with good E-values in the PSI-BLAST searches but, after it was found that they added noise to the eukaryotic searches, they were excluded. The plant RLKs were first aligned together and then the malectin-like domains excised and aligned to the animal domains using Clustal X profile alignment. A composite alignment is shown in supplementary Figure S1A and indicates a few well-conserved residues shared by plants and animals. These raise the possibility of a partially conserved function. However, the aromatic residues in the glucose disaccharide-binding pocket (Fig. 4 C and D) are not conserved.

Online resources were examined for any hint that the human KIAA0152 gene was associated with inherited disease. Neither OMIM (Hamosh et al., 2005) nor Gene2Disease (Perez-Iratxeta et al., 2002) contained information on the gene. A literature survey with 12q24.31 (the malectin locus) revealed that the lifestyle-affected, often interlinked conditions of obesity and type II diabetes have both been mapped to 12q24 (Mahtani et al., 1996, Wilson et al., 2006), sometimes to 12q24.31 (reviewed in Florez et al., 2003). The 12q24 gene for the transcription factor HNF1alpha is responsible for an early onset variant of diabetes termed MODY3, but is excluded from the NIDDM2 variant (OMIM:601407) also located at 12q24. The NIDDM2 gene has not been identified, suggesting that the causative gene (or genes) is non-obvious, and may possibly be one of the orphan genes within this region of chromosome12.

cDNA library screen and whole mount *in situ* hybridization

The original *X. laevis* malectin full-length cDNA clone was isolated from an adult pancreas cDNA library (Afelik et al., 2004). Aiming at the identification of new marker genes expressed in the pancreas, 192 clones from this λZAP Express phage cDNA library (Stratagene) were randomly picked and plasmids used for antisense RNA generation to study their spatial distribution in *Xenopus laevis* embryos by whole mount in situ hybridization (WMISH). One of them (originally termed p150) was further investigated in the context of pancreas organogenesis. It has been renamed malectin in this study. The spatial distribution of malectin transcripts in *X.laevis* embryos was determined by WMISH following standard procedures (Harland 1991, with modifications according to Hollemann et al., 1998). For this purpose, the original clone obtained from the cDNA library, pBK-CMV-p150, was linearised with BamHI and digoxigenin (Roche) labeled antisense RNA was transcribed with T7 RNA-polymerase. Transcripts were purified using the *illustra*^{TM} *RNAspin Mini Kit* (GE healthcare). Embryos were cleared in 50% formamide/ 5xSSC/ 1% H_2O_2 before imaging.

Expression constructs for structure determination and interaction studies

The open reading frame of malectin was subcloned by PCR from the full-length cDNA obtained in the pancreatic library screen (Afelik et al. 2004) into the pCS2+ eukaryotic expression vector. The malectin construct (globular segment, AA 27-213) was cloned into a modified pET-24d vector containing a N-terminal His_6-tag fused to a Z-tag removable through cleavage with TEV protease for NMR-related studies. It was expressed in *E. coli* BL21 [DE3] and purified on Ni-NTA-agarose with a subsequent cleavage of the fusion tag by TEV-protease and a second purification step on Ni-NTA-agarose.

To determine whether the recombinant protein was monomeric at the high concentrations used in the NMR experiments, we performed an analytical run on a gel filtration column and included 2% maltose in the buffer. Under these conditions the protein eluted at the expected molecular weight. ^{1}H-T2 measurements showed that the free protein is also monomeric.

Saturation transfer difference (STD) experiments

All sugars for NMR studies were purchased from Sigma-Aldrich with exception of mannobiose (Manβ1-4Man), which was purchased from Megazyme, and nigerose which was purchased from COSMO BIO CO., LTD.

The spectra were measured using a pulse sequence in which the difference between the on- and off-resonance experiments was created by phase cycling (Mayer and Meyer, 1999). Presaturation of the protein NMR signals was performed using a train of selective Gaussian pulse of a duration of 49 ms field-strength of 75 Hz each and separated by a short delay of 1ms.

Oligosaccharides and oligosaccharide probes and microarray analyses

Laminarin oligosaccharides, di-, tri- and tetrasaccharides were from Dextra (Reading, UK), penta and hexasaccharides (Megazyme,Wicklow, Ireland), and heptasaccharide (Seikagaku America, Falmouth, MA). Nigerose was from Wako Chemicals (Neuss, Germany). Cellobiose, kojibiose and maltooligosaccharides, di- to heptasaccharides were from Sigma. Tri- to hexasaccharides of cellulose were separated by gel filtration chromatography from a cellooligosaccharide mixture (V-labs purchased via Dextra). Partial depolymerizations of pustulan (Calbiochem) and dextran (Pharmacia) were performed by acetolysis and acid hydrolysis, respectively, and their fragments, di- to heptasaccharides, were fractionated by gel filtration (Palma et al., 2006). The molecular masses of the main components of oligosaccharide fractions from gel filtration were corroborated by MALDI-MS.

The high mannose *N*-glycan, $Man_7GlcNAc_2$, was a gift from Dr VE Piskarev (Moscow) and $Man_9GlcNAc_2$ was from Dextra. Glc_3Man_7(D1)GlcNAc was recovered from Glc_3Man_7 (D1)$GlcNAc_2$ that was prepared for NMR residual dipolar coupling measurements using filamentous bacteriophages (Pf1). Glc_3Man_7(D1)$GlcNAc_2$ was isolated from the glycoprotein HIV-IIIB gp120 secreted by CHO cells treated with the α-glucosidase inhibitor *N*-butyl deoxynojirimycin, as described previously (Petrescu et al., 1997). The loss of one GlcNAc unit from the original material was attributed to residual endoglycosidase activity present in the bacteriophages. The Glc_2Man_7(D1)GlcNAc was obtained from the Glc_3Man_7(D1)GlcNAc isomer [(one of three isomers D1, D2 and D3 (Petrescu et al., 1997)] by digestion with α-glucosidase I at 37°C until completion (Alonzi et al., 2007). $Glc_1Man_9GlcNAc_2$ was isolated from hen egg yolk IgY using a similar procedure to that previously reported by Ohta et al. (1991). These oligosaccharides and the gluco-oligosaccharides were converted to oxime-linked neoglycolipids (AO-NGLs) and their molecular masses were corroborated by MALDI-MS as described (Liu et al., 2007). The molecular ions for the AO-NGLs for Glc_3Man_7(D1)GlcNAc, and $Glc_1Man_9GlcNAc_2$ were exclusively mz 2559.3 and 2762.3, respectively; and for Glc_2Man_7(D1)GlcNAc mz 2396.8 with minor ions as for the parent glycan, Glc_3Man_7(D1)GlcNAc.

Microarrays of 335 lipid-linked oligosaccharide probes, NGL and glycolipids (supplemental Table S6), were robotically generated as described (Palma et al., 2006). Unless otherwise stated the NGLs were prepared by reductive amination (Chai et al., 2003).

Microarray analyses with his-tagged malectin were performed essentially as described (Palma et al., 2006), except that the protein was pre-complexed with mouse monoclonal anti-poly-histidine (Ab1) and biotinylated anti-mouse IgG antibodies (Ab2) (both from Sigma) in a ratio of 1:3:3 (by weight). In brief, the malectin-antibody complexes were prepared by pre-incubating Ab1 with Ab2 for 15 min at ambient temperature, followed by addition of malectin and incubation for a further 15 min. The malectin-antibody complexes were diluted in casein (Pierce) containing 1% (w/v) bovine serum albumin (Sigma) and 10 mM $CaCl_2$, to give a final malectin concentration of 20, 5, 1 or 0.5 μg/ml. Microarray analysis with biotinylated Concanavalin A (ConA) from Vector Laboratories (at 10 μg/ml) was performed as described (Liu et al., 2007). Binding was detected with Alexa Fluor-647-labelled streptavidin (Molecular Probes) and imaging was as described (Palma et al., 2006). Data analysis was performed with a dedicated software (Mark P. Stoll of the Glycosciences Laboratory, unpublished).

Supplemental References

Afelik, S., Chen, Y., and Pieler, T. (2004). Pancreatic protein disulfide isomerase (XPDIp) is an early marker for the exocrine lineage of the developing pancreas in Xenopus laevis embryos. Gene Expr Patterns *4*, 71-76.

Alonzi, D.S., Neville, D.C., Lachmann, R.H., Dwek, R.A., and Butters, T.D. (2007). Glucosylated free oligosaccharides are biomarkers of endoplasmic reticulum α-glucosidase inhibition. Biochem. J. *409*, 571-580.

Chai, W., Stoll, M.S., Galustian, C., Lawson, A.M. and Feizi, T. (2003). Neoglycolipid technology - deciphering information content of glycome. Methods Enzymol. *362*, 160-195.

Chenna, R., Sugawara, H., Koike, T., Lopez, R., Gibson, T.J., Higgins, D.G., and Thompson, J.D. (2003). Multiple sequence alignment with the Clustal series of programs. Nucleic Acids Res. *31*, 3497-3500.

Emanuelsson, O., Brunak, S., von Heijne, G., and Nielsen, H. (2007). Locating proteins in the cell using TargetP, SignalP and related tools. Nat Protoc. *2,* 953-971.

Florez, J.C., Hirschhorn, J., and Altshuler, D. (2003). The inherited basis of diabetes mellitus: implications for the genetic analysis of complex traits. Annu Rev Genomics Hum Genet. *4*, 257-291.

Galtier, N., Gouy, M., and Gautier, C. (1996) SEAVIEW and PHYLO_WIN: two graphic tools for sequence alignment and molecular phylogeny. Comput. Appl. Biosci. *12*, 543-548.

Harland, R.M. (1991). In situ hybridization: an improved whole-mount method for Xenopus embryos. Methods Cell. Biol. *36*, 685-695.

Hollemann, T., Chen, Y., Grunz, H. and Pieler, T. (1998) Regionalized metabolic activity establishes boundaries of retinoic acid signalling. EMBO J. *17*, 7361-7372.

Hamosh, A., Scott, A.F., Amberger, J.S., Bocchini, C.A., and McKusick, V.A. (2005) Online Mendelian Inheritance in Man (OMIM), a knowledgebase of human genes and genetic disorders. Nucleic Acids Res. *33* (Database issue), D514-517.

Letunic, I., Copley, R.R., Pils, B., Pinkert, S., Schultz, J., and Bork, P. (2006) SMART 5: domains in the context of genomes and networks. Nucleic Acids Res. *34*, D257-260.

Liu, Y., Feizi, T., Campanero-Rhodes, M.A., Childs, R.A., Zhang, Y., Mulloy, B., Evans, P.G., Osborn, H.M., Otto, D., Crocker, P.R., and Chai, W. (2007). Neoglycolipid probes prepared via oxime ligation for microarray analysis of oligosaccharide-protein interactions. Chem Biol. *14*, 847-859.

Mahtani, M.M., Widén, E., Lehto, M., Thomas, J., McCarthy, M., Brayer, J., Bryant, B., Chan, G., Daly, M., Forsblom, C., Kanninen, T., Kirby, A., Kruglyak, L., Munnelly, K., Parkkonen, M., Reeve-Daly, M.P., Weaver, A., Brettin. T., Duyk, G., Lander, E.S., and Groop, L.C. (1996). Mapping of a gene for type 2 diabetes associated with an insulin secretion defect by a genome scan in Finnish families. Nat Genet. *14*, 90-94.

Mayer, M., and Meyer, B. (1999). Characterization of Ligand Binding by Saturation Transfer Difference NMR Spectra. Angew. Chem. Int. Ed. *38*, 1784-1788.

Niehrs, C., Steinbeisser, H., and DeRobertis, E.M. (1994) Mesodermal patterning by a gradient of the vertebrate homeobox gene goosecoid. Science *263*, 817-820.

Ohta, M., Hamako, J., Yamamoto, S., Hatta, H., Kim, M., Yamamoto, T., Oka, S., Mizuochi, T., and Matsuura, F. (1991) Structures of asparagine-linked oligosaccharides from hen egg-yolk antibody (IgY). Occurence of unusual glucosylated oligo-mannose type oligosaccharides in a mature glycoprotein. Glycoconj. J**.** *8*, 400-413.

Palma, A.S., Feizi, T., Zhang, Y., Stoll, M.S., Lawson, A.M., Díaz-Rodríguez, E., Campanero-Rhodes, M.A., Costa, J., Gordon, S., Brown, G.D., and Chai, W. (2006). Ligands for the beta-glucan receptor, Dectin-1, assigned using "designer" microarrays of oligosaccharide probes (neoglycolipids) generated from glucan polysaccharides. J. Biol. Chem. *281*, 5771-5779.

Perez-Iratxeta, C., Bork, P., and Andrade, M.A. (2002). Association of genes to genetically inherited diseases using data mining. Nat Genet. *31*, 316-319.

Petrescu, A.J., Butters, T.D., Reinkensmeier, G., Petrescu, S., Platt, F.M., Dwek, R.A., and Wormald, M.R. (1997). The solution NMR structure of glucosylated N-glycans involved in the early stages of glycoprotein biosynthesis and folding. EMBO J. *16*, 4302-4310.

Sonnhammer, E.L., von Heijne, G., and Krogh, A. (1998). A hidden Markov model for predicting transmembrane helices in protein sequences. Proc. Int. Conf. Intell. Syst. Mol. Biol. *6*, 175-182.

Wilson, S.G., Adam, G., Langdown, M., Reneland, R., Braun, A., Andrew, T., Surdulescu, G.L., Norberg, M., Dudbridge, F., Reed, P.W., Sambrook, P.N., Kleyn, P.W., and Spector, T.D. (2006). Linkage and potential association of obesity-related phenotypes with two genes on chromosome 12q24 in a female dizygous twin cohort. Eur J Hum Genet. *14*, 340-348.

Supplemental results
Fig S1

A

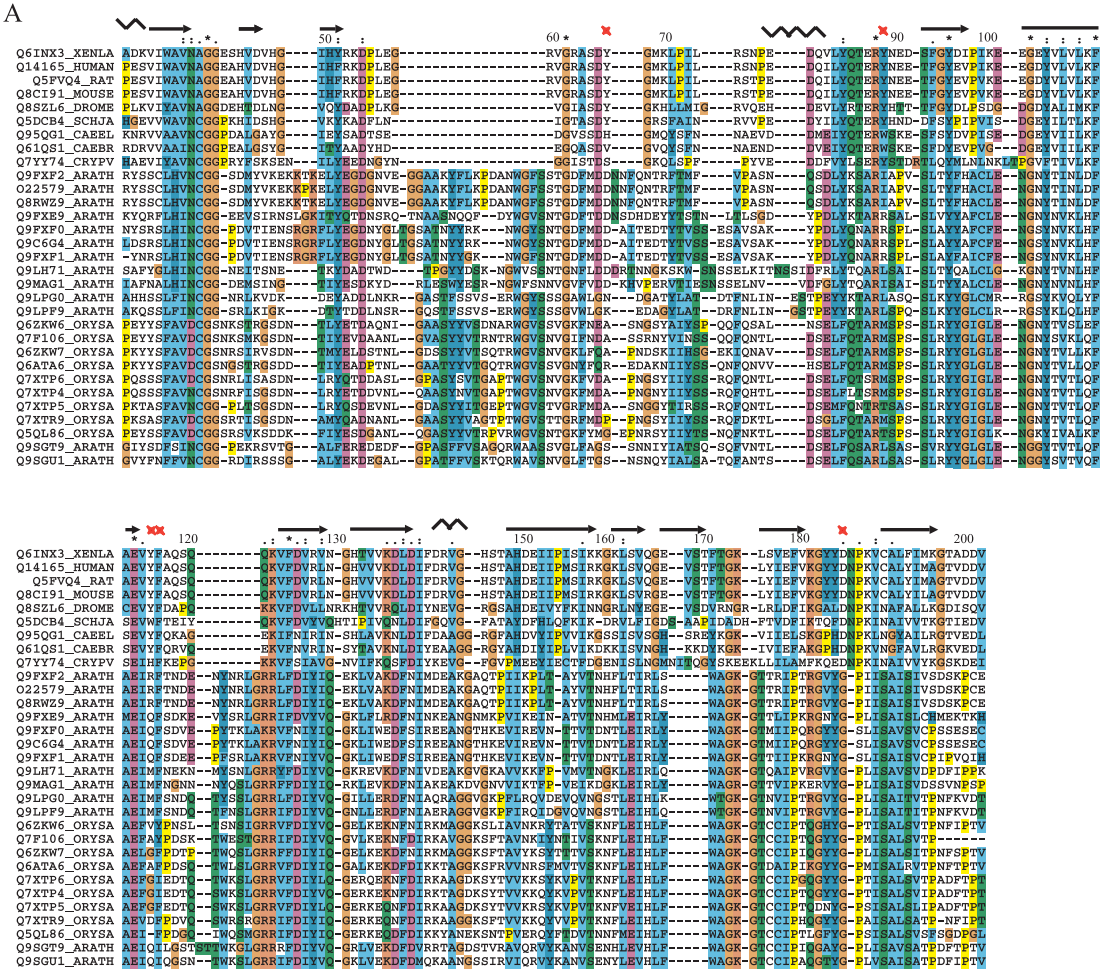

B

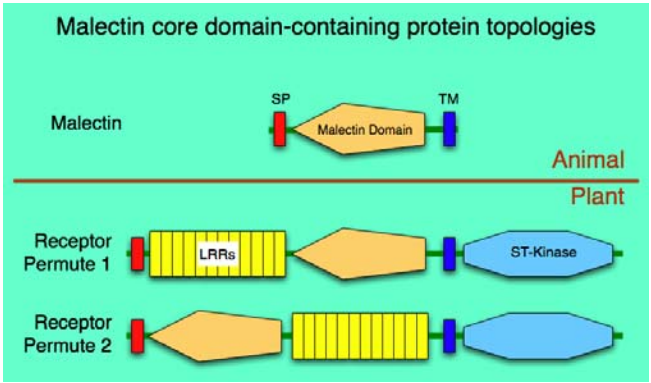

Figure S1: **Sequence alignment of animal malectin proteins vs. *Arabidopsis thaliana* and *Oryza sativa* RLK proteins.** (A) Alignment of representative arabidopsis and rice RLK-malectin-like domains with the malectin core domain of *X. laevis*, humans, rat and mouse. Sequences are labelled with UniProtKB/TrEMBL accession numbers. (XENLA = *Xenopus laevis*, DROME = *Drosophila melanogaster*, SCHJA = *Schistosoma japonicum*, CAEEL = *Caenorhabditis elegans*, CRYPV =

Cryptospridium parvum, ARATH = *Arabidopsis thaliana*, ORYSA = *Oryza sativa*). The aromatic residues and the aspartate that in *X. laevis* mediate interactions with the glucose residues (Fig.4D) are marked by red crosses, and are not conserved in plants. (B) Domain topologies of plant and animal proteins that contain the malectin core domain. The two topologies among plant RLKs are shown. Labels: SP - signal peptide; TM- transmembrane helix; LRR - leucine rich repeat: ST-Kinase – serine/threonine receptor-like kinase.

Fig S2

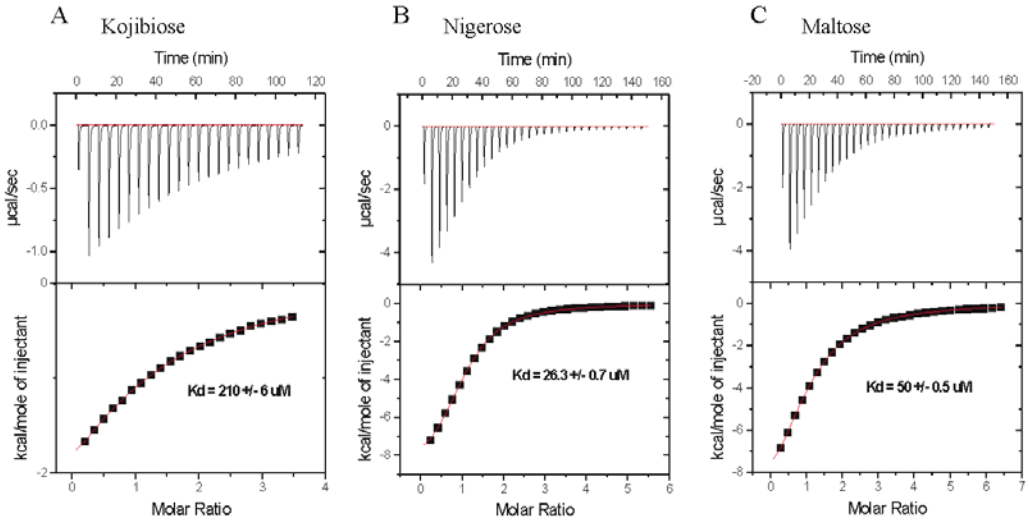

Figure S2: Malectin binding to glucose disaccharides studied by isothermal titration calorimetry. Kojibiose (A), nigerose (B) and maltose (C). The raw data are shown in the upper panel, and the integrated heat data, corrected for dilution, are shown in the lower panel.

ITC measurements were carried out using a VP-ITC Mircocal clorimeter (Mircocal, Northhampton, MA, USA) in 20mM phosphate buffer (pH 6.8), 150mM KCl and 1mM TCEP. A typical titration consisted of injecting 10µl of the sugar into the malectin sample, at time intervals of 5min, to ensure that the titration peak returned to the baseline.

Fig S3

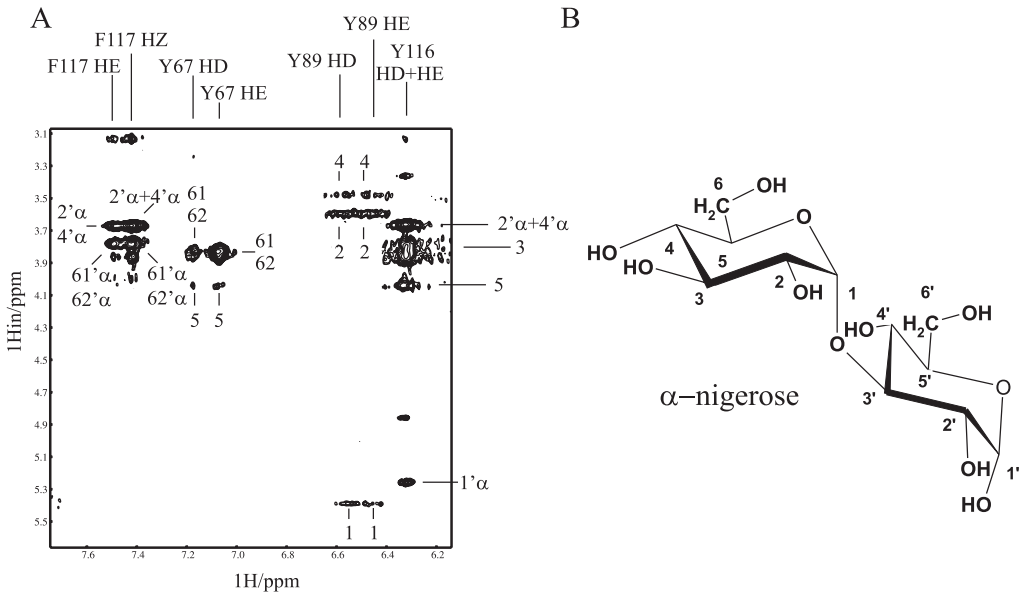

Figure S3: NOEs between malectin and nigerose. (A) Part of a ^{13}C-edited half-filtered-NOESY experiment (mixing time 150 ms) showing intermolecular NOEs between malectin and nigerose. (B) Structure of α-nigerose.

Fig S4

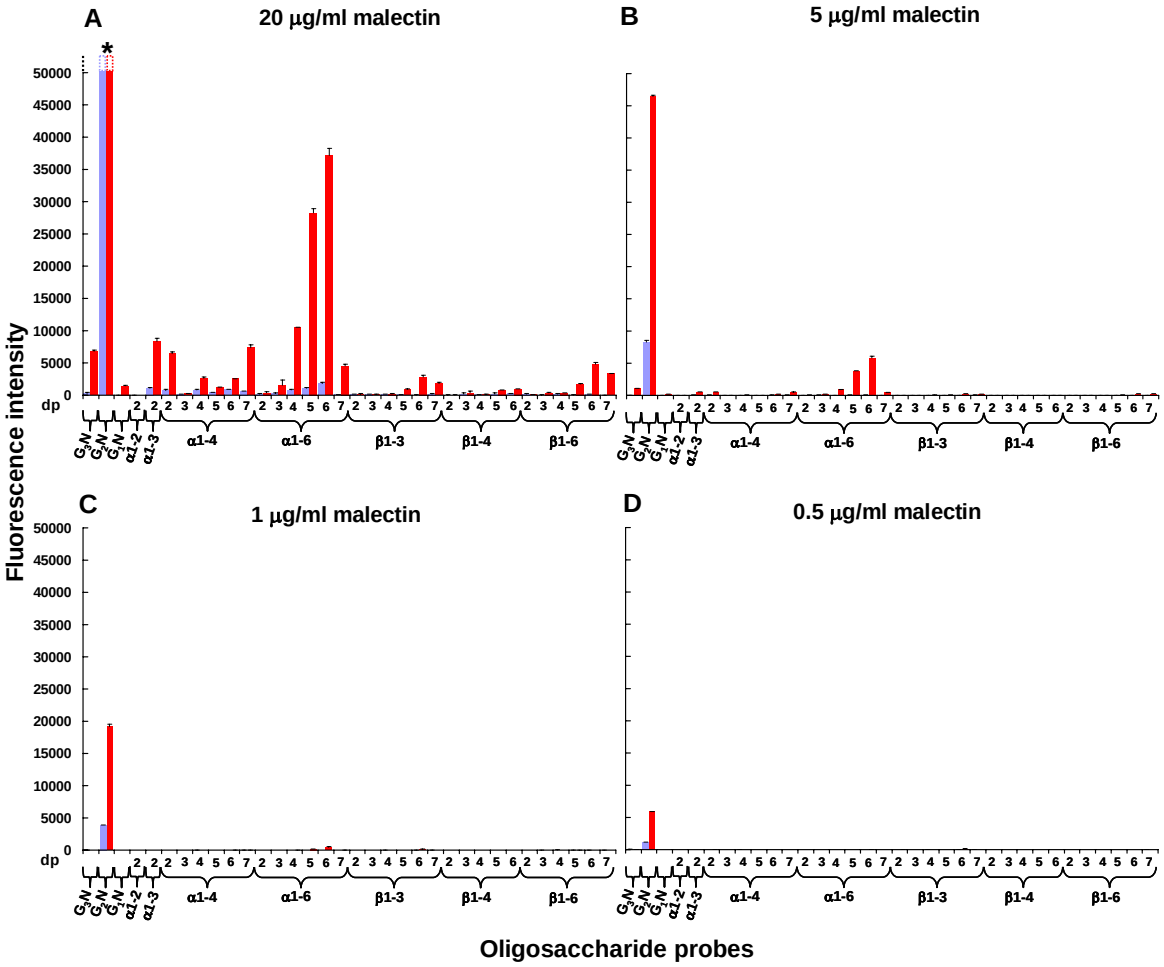

Figure S4: Microarray analyses of the interactions of malectin with Glc_1-, Glc_2- and Glc_3-high mannose *N*-glycans and gluco-oligosaccharide probes. The oligosaccharide probes were printed as duplicate spots and binding was assayed with malectin at 20, 5, 1 and 0.5 µg/ml (panels A to D, respectively). Numerical scores are shown for the binding signals [means of duplicate values at 2 and 7 fmol/spot, (blue and red bars, respectively) with error bars]. At a malectin concentration of 20 µg/ml, the binding signals for the Glc_2-high mannose *N*-glycan probe, both at 2 and 7 fmol, were too high to be accurately quantified (asterisk in A) and were annotated as >> 50000 in Table 1. Other oligosaccharide probes tested included the glucose disaccharides kojibiose (Glcα1-2Glc) nigerose (Glcα1-3Glc), maltodextrins (Glcα1-4Glc, dp 2-7); and oligosaccharides from dextran (isomalto) (Glcα1-6Glc, dp 2-7); laminarin (Glcβ1-3Glc, dp 2-7); cellulose (Glcβ1-4Glc, dp 2-6); and pustulan (Glcβ1-6Glc, dp 2-7). Abbreviations G_3N, G_2N and G_1N designate $Glc_3Man_7(D1)GlcNAc$, $Glc_2Man_7(D1)GlcNAc$ and $Glc_1Man_9GlcNAc_2$ *N*-glycan probes, respectively; dp, degree of polymerization of the gluco-oligomers.

Table S1: Structural statistics of malectin

	<SA>[a]	<SA^{watref}>[a]
A. number of structural restraints		
All NOE (unambiguous/ambigious)	4426/0	4426/0
Intraresidual	1320	1320
Sequential (|i-j|=1)	869	869
Medium-range (1<|i-j|≤ 4)	456	456
Long-range (|i-j|>4)	1781	1781
Dihedral angles $\phi\psi$	99/99	99/99
Hbonds	66	66
B. rmsd (Å) from experimental restraints[b]		
All distance restraints	0.018±0.000	0.025±0.001
Dihedral angles[c]	1.42±0.085	1.65±0.10
C. coordinate precision (Å)[d]		
N,C^{α},C'	1.04±0.19	1.12±0.17
All heavy atoms	1.94±0.28	1.96±0.26
D. structural quality[e]		
Bad contacts	12.2±3.8	2.1±1.7
Ramachandran plot (%)		
Most favored region	61.1±3.0	68.8±1.7
Additionally allowed region	32.0±3.5	24.3±2.0
Generously allowed	4.8±1.9	4.6±1.9
Disallowed	2.0±1.2	2.4±0.7

[a] <SA> is an ensemble of ten lowest-energy solution structures (out of 100 calculated) of malectin (AA28-201) before water-refinement, <SA^{watref}> is the <SA> ensemble after refinement in a shell of water (Linge et al., Methods Enzymol. 339,71-90, 2001). The CNS E_{repel} function was used to simulate van der Waals interactions with an energy constant of 25 kcal mol^{-1} $Å^{-4}$ using "PROLSQ" van der Waals radii; Rms deviations for bond length, bond angles and improper dihedral angles are 0.0023 (±0.0001) Å, 0.426 (±0.012)° and 0.365 (±0.015)° before and 0.0055 (±0.0002) Å, 0.782 (±0.043)° and 2.15 (±0.21)° after water-refinement. 1kcal=4.18kJ.

[b]Distance restraints were employed with a soft square-well potential using an energy constant of 50 kcal mol^{-1} $Å^{-2}$. No distance restraint in the <SA>[a] was violated by more than 0.2 Å.

[c]Dihedral angle restraints derived from TALOS (Cornilescu et al., J. Biomol. NMR *13*, 289-302, 1999) were applied to ϕ,ψ backbone angles using energy constants of 200 kcal mol^{-1} rad^{-2}.

[d]Coordinate precision is given as the Cartesian coordinate r.m.s. deviation of the ten lowest-energy structures in the NMR ensemble with respect to their mean structure for residue 28 to 201.

[e]Structural quality was analyzed using PROCHECK.

Table S2: Domains having the highest structural similarity to malectin. The most similar structures in the PDB data bank identified by a search with MSD-Fold (www.ebi.ac.uk/msd-srv/ssm/) were the structures of the carbohydrate-binding modules (CBMs) of bacterial glycosylhydrolases (representatives of different families are shown) and the carbohydrate recognition domain of a ubiquitin ligase, Fbs1,. Their reported ligands are also shown.

domain/PDB	z-score	RMSD (Å)	seq-ID(%)	ligand	species
CBM22 (1dyo)	7.3	3.2	9	Xylan	C*lostridium thermocellum*
Fbs1 CRD (1umh)	7.2	2.9	7	Chitobiose	*Mus musculus*
CBM22 (1h6y)	7.2	3.2	10	Xylan	*Clostridium thermocellum*
CBM22 (1h6x)	7.2	3.3	9	Xylan	*Clostridium thermocellum*
CBM35 (2bgp)	6.6	2.8	14	Mannan	*Clostridium japonocus*
CBM6 (1uz0)	6.3	3.7	11	Cellubiose	*Clostridium mixtus*
CBM27 (1pmj)	6.1	3.3	12	Mannan	*Clostridium sacharolyticum*
CBM27 (1pmh)	6.0	3.3	10	Mannan	*Clostridium sacharolyticum*
CBM15 (1gny)	6.0	3.4	12	Xylan	*Pseudomonas cellulosa*
CBM4 (1k45)	6.0	3.0	9	Xylan	*Rhodothermus marinus*

PDB = protein data bank accession code, seq-ID = overall sequence identity

Table S3: Carbohydrate-malectin interaction screen by NMR. Interactions were determined through ^{15}N-chemical shift perturbation experiments. Relative affinities of oligosaccharides bound were determined through STD experiments.

Carbohydrate	binding to malectin
D-sialic acid	–
L-fucose	–
D-glucose	–
D-*N*-acetyl-glucosamine	–
D-galactose	–
D-mannose	–
fructose	–
D-*N*-acetyl-galactosamine	–
lactose (Galβ1-4Glc)	–
sucrose (Glcα1-2Fruc)	–
chitobiose (GlcNAcβ1-4GlcNAc)	–
trehalose (Glcβ1-1Glc)	–
mannobiose (Manα1-3Man)	–
mannobiose (Manβ1-4Man)	–
3'-siayllactose (NeuAcα2,3Galβ1-4Glc)	–
maltose (Glcα1-4Glc)	++
maltotriose (Glcα1-4Glcα1-4Glc)	++
maltotetraose (Glcα1-4Glcα1-4Glcα1-4Glc)	++
maltoheptaose (Glcα1-4Glcα1-4Glcα1-4Glcα1-4Glcα1-4Glcα1-4Glc)	++
kojibiose (Glcα1-2Glc)	+
nigerose (Glcα1-3Glc)	++
isomaltose (Glcα1-6Glc)	++
cellobiose (Glcβ1-4Glc)	+

– an interaction was not observed in chemical shift perturbation experiments;
\+ an interaction was observed in chemical shift perturbation experiments, but the STD signals were weak
++ an interaction was observed in chemical shift perturbation experiments and the STD signals were strong

Table S4: Chemical shift assignment of the disaccharides investigated by STD. The reducing end glucose rings exist in two isomeric forms in equilibrium, α and β according to the chirality of the anomeric centre. In the case of the disaccharides maltose, cellobiose, and isomaltose, the proton resonances of the non-reducing end glucose ring are fully overlapping, whereas the frequencies of the protons of the reducing end glucose ring are clearly separated. For nigerose and kojibiose, protons of the non-reducing end glucose also display two sets of resonances for the two isomers.

	Maltose				***Cellobiose***			
	α		β		α		β	
	^{1}H	^{13}C	^{1}H	^{13}C	^{1}H	^{13}C	^{1}H	^{13}C
1	5.382	99.69	5.382	99.69	4.485	102.72	4.485	102.72
2	3.551	71.81	3.551	71.81	3.291	73.34	3.291	73.34
3	3.651	72.95	3.651	72.95	3.481	75.64	3.481	75.64
4	3.389	69.42	3.389	69.42	3.463	76.13	3.463	76.13
5	3.693	72.77	3.693	72.77	3.393	69.60	3.393	69.60
6	3.825 3.732	60.592	3.825 3.732	60.592	3.892 3.709	60.71	3.892 3.709	60.71
1'	5.198	92.02	4.622	95.88	5.197	91.91	4.636	95.91
2'	3.537	71.42	3.243	74.12	3.549	71.36	3.245	74.03
3'	3.939	73.38	3.738	76.30	3.795	71.45	3.620	78.72
4'	3.617	76.97	3.615	76.76	3.615	78.84	3.597	74.44
5'	3.911	70.06	3.567	74.69	3.921	70.29	3.570	74.94
6'	3.799	60.71	3.881 3.736	60.85	3.848	60.04	3.929 3.782	60.19

	Nigerose				***Kojibiose***			
	α		β		α		β	
1	5.361	99.05	5.347	98.99	5.091	96.43	5.381	97.87
2	3.561	71.65	3.554	71.60	3.549	71.54	3.538	71.58
3	3.753	72.86	3.734	72.91	3.783	72.9	3.744	72.94
4	3.435	69.41	3.453	69.25	3.450	69.56	3.456	69.47
5	4.000	71.71	4.007	71.65	3.939	71.95	4.027	71.78
6	3.816 3.765	60.36	3.797	60.19	3.835 3.775	60.48	3.800	60.41
1'	5.226	92.19	4.656	95.93	5.433	89.57	4.791	96.38
2'	3.626	70.07	3.327	72.80	3.630	76.04	3.378	78.68
3'	3.841	79.58	3.630	82.15	3.810	71.37	3.565	74.59
4'	3.626	70.07	3.640	70.02	3.453	69.72	3.422	69.89
5'	3.843	71.16	3.567	75.59	3.855	71.45	3.456	75.87
6'	3.837 3.747	60.37	3.878 3.711	60.54	3.840 3.762	60.72	3.890 3.710	60.94

	Isomaltose			
	α		β	
1	4.932	98.07	4.932	98.07
2	3.531	71.63	3.531	71.63
3	3.713	73.25	3.713	73.25
4	3.405	69.62	3.405	69.62
5	3.710	71.91	3.710	71.91
6	3.826 3.741	60.59	3.826 3.741	60.59
1'	5.218	92.37	4.650	96.25

	Isomaltose			
2'	3.527	71.57	3.228	74.19
3'	3.685	73.19	3.459	76.14
4'	3.493	69.68	3.494	69.50
5'	3.986	70.14	3.616	74.44
6'	3.973 3.675	65.88	3.932 3.733	65.83

Table S5: Structural statistics of the malectin-nigerose complex

	$<SA^{nigerose}>^{a}$
A. number of structural restraints	
All NOE (unambiguous/ambigious)	4458/0
Protein to protein	4427
Protein to sugar	31
Intraresidual	1320
Sequential (|i-j|=1)	869
Medium-range (1<|i-j|≤ 4)	456
Long-range (|i-j|>4)	1782
Dihedral angles $\phi\psi$	99/99
Hbonds	66
B. rmsd (Å) from experimental restraints[b]	
All distance restraints	0.033±00.3
Dihedral angles[c]	1.92±0.08
C. coordinate precision (Å)[d]	
N,C^{α},C'	0.92±0.16
All heavy atoms	1.77±0.18
D. structural quality[e]	
Bad contacts	14.0±2.6
Ramachandran plot (%)	
Most favored region	63.8±2.2
Additionally allowed region	28.8±2.6
Generously allowed	4.8±2.0
Disallowed	2.7±0.8

[a] $<SA^{nigerose}>$ is an ensemble of ten lowest-energy solution structures (out of 100 calculated) of the malectin nigerose complex (AA28-201) before water-refinement. The CNS E_{repel} function was used to simulate van der Waals interactions with an energy constant of 25 kcal mol^{-1} $Å^{-4}$ using "PROLSQ" van der Waals radii; Rms deviations for bond length, bond angles and improper dihedral angles are 0.0023 (±0.0001) Å, 0.426 (±0.012)° and 0.365 (±0.015)° before water-refinement. 1kcal=4.18kJ.

[b]Distance restraints were employed with a soft square-well potential using an energy constant of 50 kcal $mol^{-1}Å^{-2}$.

[c]Dihedral angle restraints derived from TALOS (Cornilescu et al., J. Biomol. NMR *13*, 289-302, 1999) were applied to ϕ,ψ backbone angles using energy constants of 200 kcal mol^{-1} rad^{-2}.

[d]Coordinate precision is given as the Cartesian coordinate r.m.s. deviation of the ten lowest-energy structures in the NMR ensemble with respect to their mean structure for residue 28 to 201.

[e]Structural quality was analyzed using PROCHECK.

Table S6: Oligosaccharide probes* included in the microarray and the binding signals (means at 7 fmol) with malectin at 5µg/ml.

Pos**	Probe Name	Sequence	Signal at 7 fmol
	Mammalian-type		
1	Glucocerebrosides	Glcß-Cer	5
2	Lac	Galß-4Glc-DH	12
3	Lac-AO	Galß-4Glc-AO	16
4	Lactocerebrosides	Galß-4Glcß-Cer	11
5	LacNAc	Galß-4GlcNAc-DH	10
6	Galß-3GalNAc	Galß-3GalNAc-DH	1
7	Galß-6GalNAc	Galß-6GalNAc-DH	10
8	GalNAcα-3Galß-4Glc	GalNAcα-3Galß-4Glc-DH	11
9	Galα-4Galß-4GlcNAc	Galα-4Galß-4GlcNAc-DH	2
10	Ceramide trihexoside	Galα-4Galß-4Glcß-Cer	<1
11	Globoside (P-antigen)	GalNAcß-3Galα-4Galß-4Glcß-Cer	3
12	Forssmann glycolipid	GalNAcα-3GalNAcß-3Galα-4Galß-4Glcß-Cer	<1
13	H-Di	Fucα-2Gal-DH	31
14	B-Tri	Galα-3Gal-DH | Fucα-2	5
15	A-Tri	GalNAcα-3Gal-DH | Fucα-2	<1
16	Lex-Tri	Galß-4GlcNAc-DH | Fucα-3	9
17	Lea-Tri	Galß-3GlcNAc-DH | Fucα-4	<1
18	GM4	NeuAcα-3Galβ-Cer	<1
19	NeuAcα-(3')Lac	NeuAcα-3Galß-4Glc-DH	31
20	NeuAcα-(6')Lac	NeuAcα-6Galß-4Glc-DH	10
21	NeuAcß-(3')Lac	NeuAcß-3Galß-4Glc-DH	7
22	NeuAcß-(6')Lac	NeuAcß-6Galß-4Glc-DH	25
23	Neuα-(3')Lac	Neuα-3Galß-4Glc-DH	10
24	Neuα-(6')Lac	Neuα-6Galß-4Glc-DH	21
25	Neu4,5Ac-(3')Lac	Neu4,5Acα-3Galß-4Glc-DH	<1
26	Neu5,9Ac-(6')LN	Neu5,9Acα-6Galß-4GlcNAc-DH	9
27	GM3	NeuAcα-3Galß-4Glcß-Cer	<1
28	GM3(Gc)	NeuGcα-3Galß-4Glcß-Cer	23
29	NeuAcα-(6')LN	NeuAcα-6Galß-4GlcNAc-DH	<1
30	Haematoside	NeuAcα-3Galß-4Glcß-Cer	<1
31	SA(3')-Lea-Tri	NeuAcα-3Galß-3GlcNAc-DH | Fucα-4	<1
32	GD3	NeuAcα-8NeuAcα-3Galß-4Glcß-Cer	<1
33	Sulfatide	SU-3Galβ-Cer	<1
34	GSF-1	SU-3Galβ-C30	15
35	GSF-19	SU-6Glcβ-C30	15
36	SM3	SU-3Galß-4Glc-DH	4
37	SU(3')-LN	SU-3Galß-4GlcNAc-DH	5
38	GSC-210	SU-3GlcAß-3Galß-Cer42	6
39	SU(3')-Lex-Tri	SU-3Galß-4GlcNAc-DH | Fucα-3	<1

40	SU(3')-Lea-Tri	SU-3Galß-3GlcNAc-DH | Fucα-4	9
41	GSC-150	SU-3Galß-4Glcß-C30 | Fucα-3	3
42	GSC-432	3-deoxy,3-carboxymethyl-Galß-4Glcß-C30	15
43	GSC-430	3-deoxy,3-carboxymethyl-Galß-3Glcß-C30 | Fucα-4	1
44	GSC-260	3-deoxy,3-carboxymethyl-Galß-4Glcß-C30 | Fucα-3	6
45	GSC-209	GlcAß-3Galß-Cer42	<1
46	Glc	Glc-DH	7
47	Gal	Gal-DH	2
48	Gal-AO	Gal-AO	15
49	LacNAc-AO	Galß-4GlcNAc-AO	11
50	NeuAcα-(3')LN	NeuAcα-3Galß-4GlcNAc-DH	<1
51	NeuAcα-(3')LN-AO	NeuAcα-3Galß-4GlcNAc-AO	<1
52	Lea-Tri-AO	Galß-3GlcNAc-AO | Fucα-4	<1
53	Lex-Tri-(Me)AO	Galß-4GlcNAc-(Me)-AO | Fucα-3	<1
54	Neu4,5Ac-(3')Lac-AO	Neu4,5Acα-3Galß-4Glc-AO	<1
55	LacN(1-3)-AO	Galß-3GlcNAc-AO	<1
56	NeuAcα-(3')Lac-AO	NeuAcα-3Galß-4Glc-AO	7
57	NeuAcα-(6')Lac-AO	NeuAcα-6Galß-4Glc-AO	<1
58	NeuAcß-(3')Lac-AO	NeuAcß-3Galß-4Glc-AO	29
59	NeuAcß-(6')Lac-AO	NeuAcß-6Galß-4Glc-AO	5
60	Neuα-(3')Lac-AO	Neuα-3Galß-4Glc-AO	19
61	Neuα-(6')Lac-AO	Neuα-6Galß-4Glc-AO	8
62	Lex-Tri-AO	Galß-4GlcNAc-AO | Fucα-3	<1
63	Galactocerebrosides	Galß-Cer	5
64	GSC-426	3-deoxy-3Ac-Galß-C30	15
65	LNT	Galß-3GlcNAcß-3Galß-4Glc-DH	10
66	LNnT	Galß-4GlcNAcß-3Galß-4Glc-DH	14
67	Paragloboside	Galß-4GlcNAcß-3Galß-4Glcß-Cer	<1
68	B-like pentaosylceramide	Galα-3Galß-4GlcNAcß-3Galß-4Glcß-Cer	<1
69	Klaus glycolipid	Galß-3Galß-4GlcNAcß-3Galß-4Glcß-Cer	5
70	LNFP-I	Fucα-2Galß-3GlcNAcß-3Galß-4Glc-DH	20
71	LNFP-III	Galß-4GlcNAcß-3Galß-4Glc-DH | Fucα-3	39
72	LNFP-II	Galß-3GlcNAcß-3Galß-4Glc-DH | Fucα-4	20
73	A-Hexa	GalNAcα-3Galß-3GlcNAcß-3Galß-4Glc-DH | Fucα-2	8
74	A-Hepta	GalNAcα-3Galß-3GlcNAcß-3Galß-4Glc-DH | | Fucα-2 Fucα-4	30

75	LNnDFH-V	Galß-4GlcNAcß-3Galß-4Glc-DH | | Fucα-3 Fucα-2	3
76	LNDFH-I	Fucα-2Galß-3GlcNAcß-3Galß-4Glc-DH | Fucα-4	<1
77	LNnDFH-I	Fucα-2Galß-4GlcNAcß-3Galß-4Glc-DH | Fucα-3	<1
78	LNnDFH-II	Galß-4GlcNAcß-3Galß-4Glc-DH | | Fucα-3 Fucα-3	<1
79	LNDFH-II	Galß-3GlcNAcß-3Galß-4Glc-DH | | Fucα-4 Fucα-3	<1
80	LNnTFH-I	Fucα-2Galß-4GlcNAcß-3Galß-4Glc-DH | | Fucα-3 Fucα-2	6
81	LNTFH-I	Fucα-2Galß-3GlcNAcß-3Galß-4Glc-DH | | Fucα-4 Fucα-2	14
82	Leb-hexaosylceramide	Fucα-2Galß-3GlcNAcß-3Galß-4Glcß-Cer | Fucα-4	<1
83	B-hexaosylceramide	Galα-3Galß-4GlcNAcß-3Galß-4Glcß-Cer | Fucα-2	22
84	LSTa	NeuAcα-3Galß-3GlcNAcß-3Galß-4Glc-DH	24
85	GSC-31	NeuAcα-3Galß-4GlcNAcß-3Galß-4Glcß-Cer36	9
86	Sialylparagloboside	NeuAcα-3Galß-4GlcNAcß-3Galß-4Glcß-Cer	<1
87	SA(3')-LNFP-II	NeuAcα-3Galß-3GlcNAcß-3Galß-4Glc-DH | Fucα-4	<1
88	SA(3')-LNFP-III	NeuAcα-3Galß-4GlcNAcß-3Galß-4Glc-DH | Fucα-3	<1
89	GSC-64	NeuAcα-3Galß-4GlcNAcß-3Galß-4Glcß-Cer36 | Fucα-3	<1
90	GSC-472	Neuα-3Galß-4GlcNAcß-3Galß-4Glcß-Cer36 | Fucα-3	<1
91	SA(3/6)LNFP-I	NeuAcα-3/6Galß-3GlcNAcß-3Galß-4Glc-DH | Fucα-2	<1
92	GSC-97	NeuAcα-6Galß-4GlcNAcß-3Galß-4Glc-Cer36 | Fucα-3	<1
93	LSTb	Galβ-3GlcNAcβ-3Galβ-4Glc-DH | NeuAcα-6	<1
94	DSLNT	NeuAcα-3Galß-3GlcNAcß-3Galß-4Glc-DH | NeuAcα-6	1
95	SU(3')-Tri	SU-3Galß-4GlcNAcß-3Gal-DH	<1
96	GSC-190	SU-3GlcAß-3Galß-4GlcNAcß-3Galß-4Glcß-Cer42	3
97	SU(3')-LNFP-II	SU-3Galß-3GlcNAcß-4Galß-4Glc-DH | Fucα-4	<1
98	SU(3')-LNFP-III	SU-3Galß-4GlcNAcß-3Galß-4Glc-DH | Fucα-3	9

99	SU(6')-LNFP-II	SU-6Galß-3GlcNAcß-3Galß-4Glc-DH Fucα-4	3
100	SU(6')-LNFP-III	SU-6Galß-4GlcNAcß-3Galß-4Glc-DH Fucα-3	7
101	SU(3',6)-LNFP-III	SU-6 SU-3Galß-4GlcNAcß-3Galß-4Glc-DH Fucα-3	4
102	GSC-268	SU-6 NeuAcα-3Galß-4GlcNAcß-3Galß-4Glc-Cer36 Fucα-3	5
103	GSC-268 deNAc	SU-6 Neuα-3Galß-4GlcNAcß-3Galß-4Glc-Cer36 Fucα-3	2
104	GSC-269	SU-6 NeuAcα-3Galß-4GlcNAcß-3Galß-4Glcß-Cer36 Fucα-3	<1
105	GSC-406	SU-6 Neuα-3Galß-4GlcNAcß-3Galß-4Glcß-Cer36 Fucα-3	15
106	GSC-270	SU-6 SU-6 NeuAcα-3Galß-4GlcNAcß-3Galß-4Glcß-Cer36 Fucα-3	<1
107	GSC-189	GlcAß-3Galß-4GlcNAcß-3Galß-4Glcß-Cer42	16
108	GSC-207	GlcAß-3Galß-4GlcNAcß-3Galß-4Glcß-C30	2
109	Led-II pentaosylceramide	Fucα-2Galß-3GlcNAcß-3Galß-4Glcß-CerA	<1
110	Led-I pentaosylceramide	Fucα-2Galß-3GlcNAcß-3Galß-4Glcß-CerB	<1
111	LNFP-III-AO	Galß-4GlcNAcß-3Galß-4Glc-AO Fucα-3	<1
112	GSC-31	NeuAcα-3Galß-4GlcNAcß-3Galß-4Glcß-Cer36	15
113	LSTc	NeuAcα-6Galβ4-GlcNAcβ3-Galβ4-Glc-DH	3
114	GSC-208	SU-3GlcAß-3Galß-4GlcNAcß-3Galß-4Glcß-C30	3
115	GSC-97	NeuAcα-6Galß-4GlcNAcß-3Galß-4Glcß-Cer36 Fucα-3	5
116	DLNN	GlcNAcß-3Galß-4Glc-DH	6
117	GSC-105	NeuAcα-3Galß-4GlcNAcß-3Galß-Cer36 Fucα-3	<1
118	GSC-516B	Neuα-3Galß-4GlcNAcß-3Galß-4Glcß-Cer36 SU-6	6
119	pLNnH	Galß-4GlcNAcß-3Galß-4GlcNAcß-3Galß-4Glc-DH	<1
120	LNnH	Galß-4GlcNAcß-6 Galß-4Glc-DH Galß-4GlcNAcß-3	3

121	LND	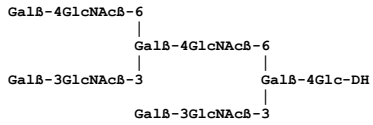	<1
122	Nonaosylceramide	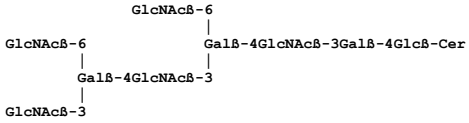	<1
123	I-dodecaosylceramide	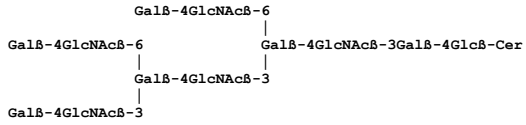	23
124	B-like pentadecaosylceramide	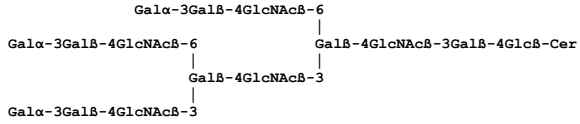	15
125	I-hexadecaosylceramide	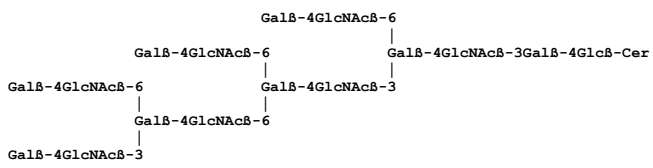	49
126	B-like eicosaosylceramide	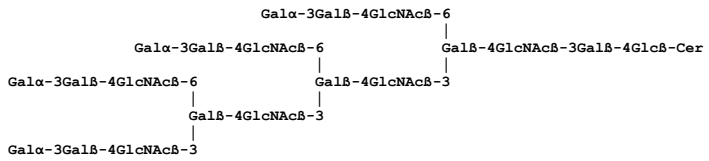	12
127	I-eicosaosylceramide	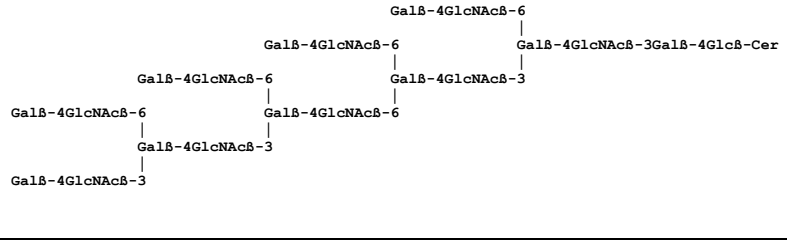	26

128	B-like pentaeicosaosylceramide	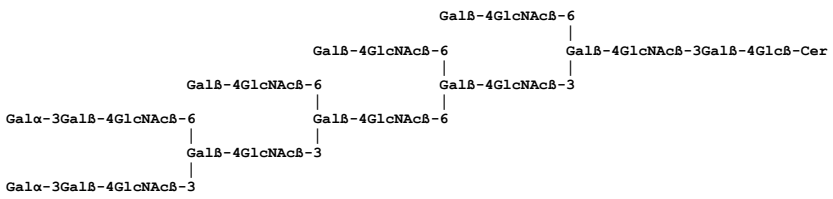	2
129	pLNFH-IV	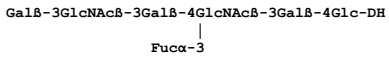	<1
130	DFpLNH-II	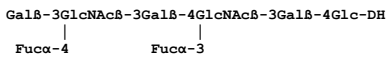	9
131	MFLNH-III		<1
132	MFLNnH(a)	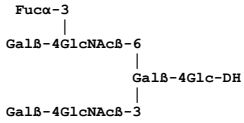	8
133	DFLNH(a)	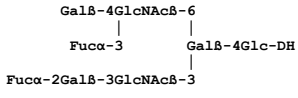	23
134	DFLNH(c)	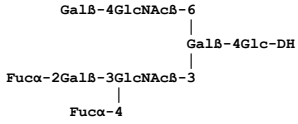	16
135	DFLNnH	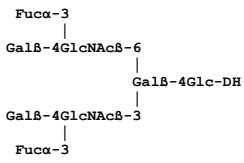	<1
136	DFLNH(b)	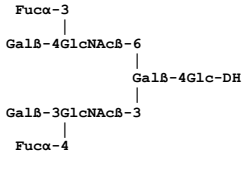	9

137	TFLNH	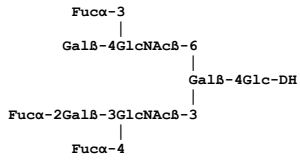	8
138	TFpLNH-I	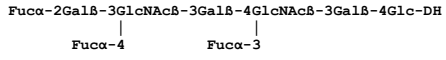	11
139	MFiLNO-IV	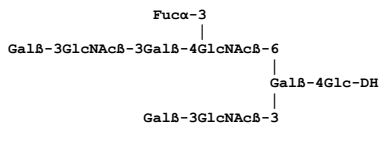	20
140	MFLND	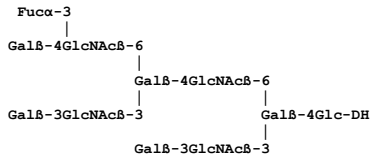	7
141	B-III dodecaosylceramide	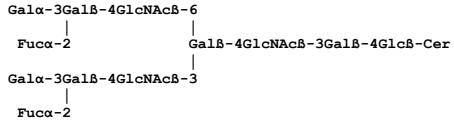	12
142	B-IV tetradecaosylceramide		<1
143	MSLNH	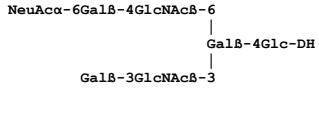	<1
144	MSLNnH-I	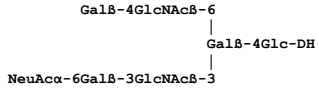	<1
145	MSMFLNH	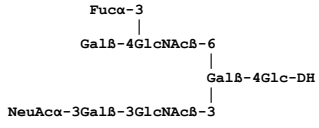	<1
146	MFMSLNnH	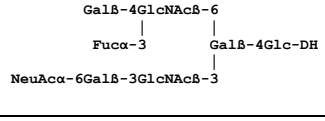	<1

147	DSLNnH	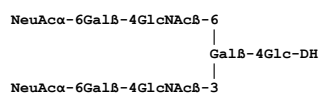	<1
148	GSC-219	SU-3GlcAß-3Galß-4GlcNAcß-3Galß-4GlcNAcß-3Galß-4Glcß-Cer36	2
149	C4U	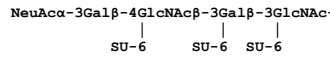	3
150	FucC4U	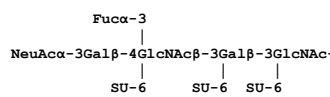	<1
151	GSC-216	GlcAß-3Galß-4GlcNAcß-3Galß-4GlcNAcß-3Galß-4Glcß-Cer42	8
152	TFiLNO	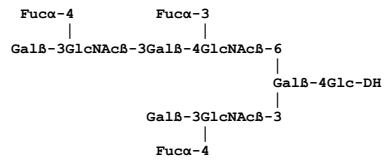	6
153	pLNH	Galß-3GlcNAcß-3Galß-4GlcNAcß-3Galß-4Glc-DH	<1
154	LNH	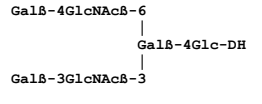	2
155	iLNO	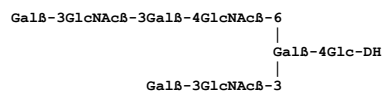	<1
156	I-octaosylceramide	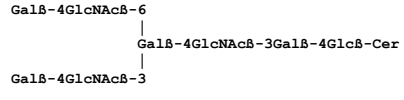	<1
157	B-like decaosylceramide	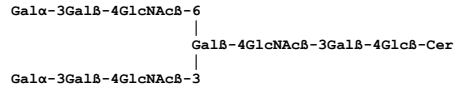	8
158	GSC-217	SU-3GlcAß-3Galß-4GlcNAcß-3Galß-4GlcNAcß-3Galß-4Glcß-Cer42	10
159	GSC-220	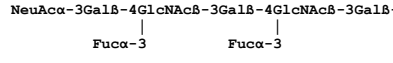	19
160	GSC-221	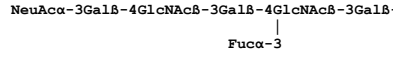	3
161	GSC-218	GlcAß-3Galß-4GlcNAcß-3Galß-4GlcNAcß-3Galß-4Glcß-Cer36	<1
162	Glc3Man7(D1)GN1-AO	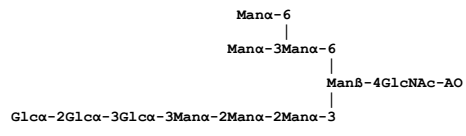	1077

163	Glc2Man7(D1)GN1-AO	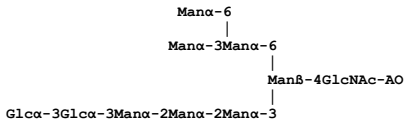	46454
164	Glc1Man9GN2-AO	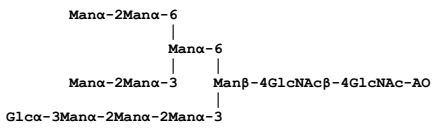	182
165	Man9GN2-AO	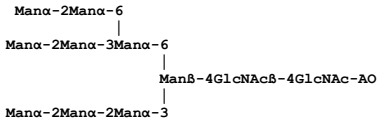	<1
166	Man8(D1D3)GN2	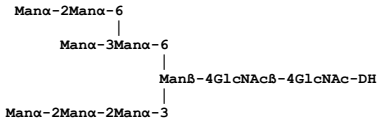	3
167	Man7(D1)GN2	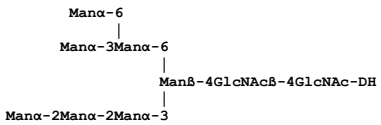	<1
168	Man7(D1)GN2-AO	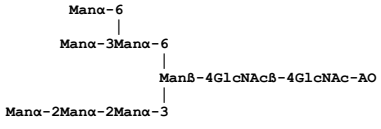	17
169	Man7(D3)GN2	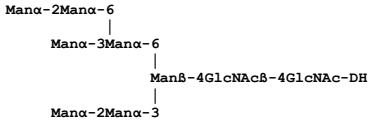	<1
170	Man6GN2	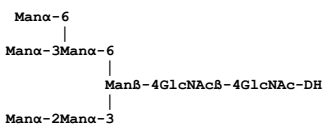	<1
171	Man5GN2	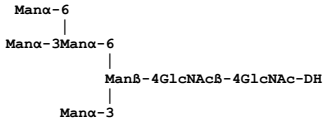	<1

172	Man4aGN2	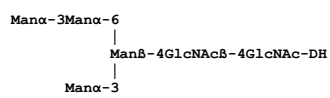	<1
173	Man4bGN2	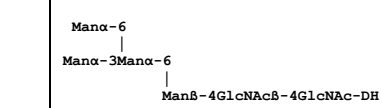	<1
174	Man3FGN2	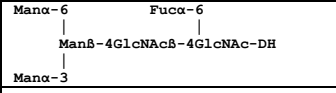	<1
175	Man3GN2	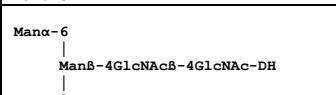	11
176	Man2aGN2	Manα-6Manß-4GlcNAcß-4GlcNAc-DH	25
177	Man2GN1	Manα-3Manß-4GlcNAc-DH	<1
178	Man1GN1	Manß-4GlcNAc-DH	1
179	N1	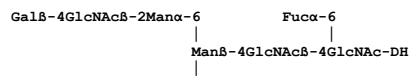	5
180	N2	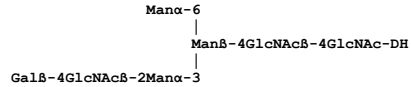	1
181	N4	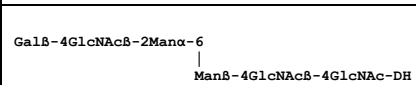	1
182	N3	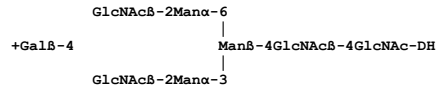	3
183	NGA2	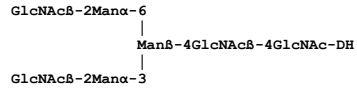	<1
184	NGA2B	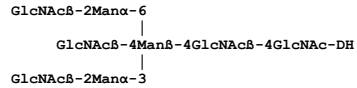	10
185	NA2	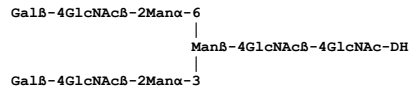	<1
186	NGA2F	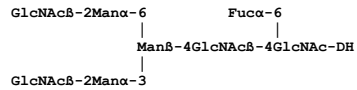	<1

187	NA2F	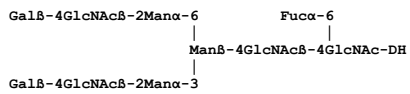	<1
188	NA2F-AO	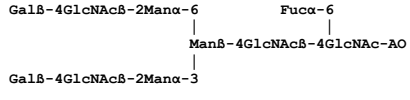	<1
189	NA2FB	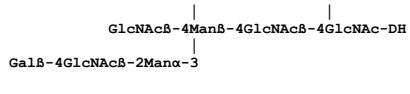	<1
190	A2(2-6)	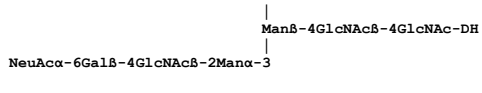	1
191	A2F(2-3)	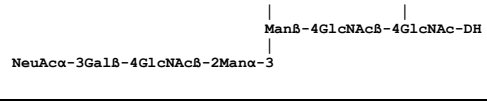	<1
192	AGP-Bi-Ac2	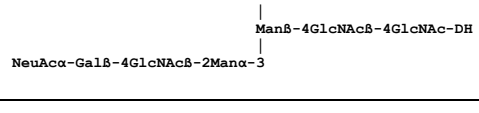	<1
193	AGP-Bi-AcGc	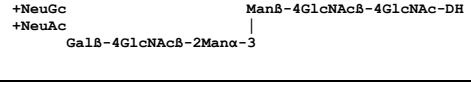	<1
194	AGP-Bi-Gc2	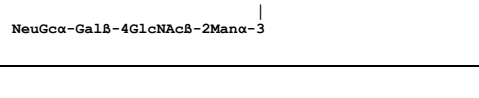	<1
195	NGA3B	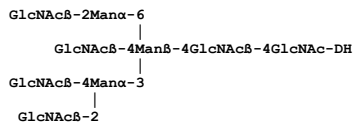	<1
196	NA3-Lex	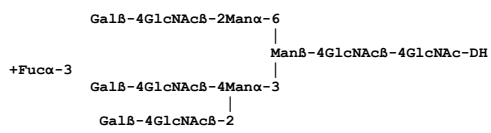	<1
197	NA3	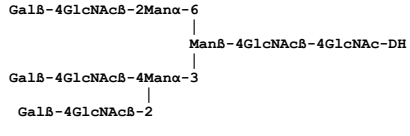	<1

198	A3	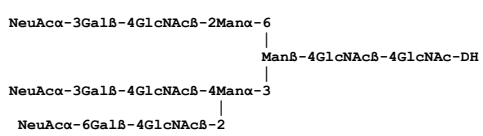	<1
199	NGA4	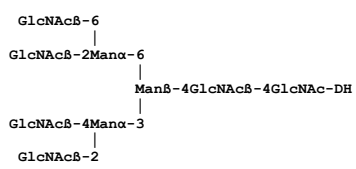	<1
200	NA4	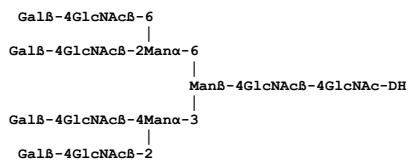	10
201	NGA5B	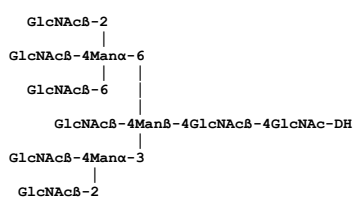	6
202	GN2-Man5BGN2	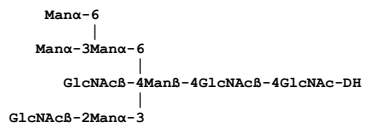	<1
203	Fuc-GlcNAc	Fucα-6GlcNAc-DH	8
204	Man3(α3,α6)		<1
205	Man5(α3,α6)	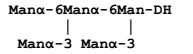	3
206	Man2(α3)	Manα-3Man-DH	<1
207	Man2(α2)	Manα-2Man-DH	<1
208	SA2(α8)	NeuAcα-8NeuAc-DH	6
209	SA3(α8)	NeuAcα-8NeuAcα-8NeuAc-DH	10
210	SA4(α8)	NeuAcα-8NeuAcα-8NeuAcα-8NeuAc-DH	6
211	SA5(α8)	NeuAcα-8NeuAcα-8NeuAcα-8NeuAcα-8NeuAc-DH***	<1
212	SA6(α8)	NeuAcα-8NeuAcα-8NeuAcα-8NeuAcα-8NeuAcα-8NeuAc-DH***	<1
213	SA7(α8)	NeuAcα-8NeuAcα-8NeuAcα-8NeuAcα-8NeuAcα-8NeuAcα-8NeuAc-DH***	<1
214	SA8(α8)	NeuAcα-8NeuAcα-8NeuAcα-8NeuAcα-8NeuAcα-8NeuAc-8NeuAcα-8NeuAc-DH***	3
215	SA9(α8)	NeuAcα-8NeuAcα-8NeuAcα-8NeuAcα-8NeuAcα-8NeuAc-8NeuAcα-8NeuAc-8NeuAcα-DH***	7
216	SA10(α8)	NeuAcα-8NeuAcα-8NeuAcα-8NeuAcα-8NeuAcα-8NeuAc-8NeuAcα-8NeuAcα-8NeuAcα-8NeuAc-DH***	<1
217	SA11(α8)	NeuAcα-8NeuAcα-8NeuAcα-8NeuAcα-8NeuAcα-8NeuAc-8NeuAcα-8NeuAαc-8NeuAcα-8NeuAcα-8NeuAc-DH***	3

218	NeuAc	NeuAc-DH	<1
219	NeuAc-AO	NeuAc-AO	<1
220	Asialo-GM2	GalNAcβ-4Galβ-4Glcβ-Cer	10
221	GalNAc-Tetra	Galß-3GalNAcß-4Galß-4Glc-DH	<1
222	Asialo-GM1	Galβ-3GalNAcβ-4Galβ-4Glcβ-Cer	3
223	GM1	Galβ-3GalNAcβ-4Galβ-4Glcβ-Cer | NeuAcα-3	<1
224	GM1(Gc)	Galβ-3GalNAcβ-4Galβ-4Glcβ-Cer | NeuGcα-3	<1
225	GM1-penta	Galβ-3GalNAcβ-4Galβ-4Glc-DH | NeuAcα-3	<1
226	GM1(Gc)-penta	Galβ-3GalNAcβ-4Galβ-4Glc-DH | NeuGcα-3	<1
227	GM2	GalNAcβ-4Galβ-4Glcβ-Cer | NeuAcα-3	<1
228	GD1a	NeuAcα-3Galß-3GalNAcß-4Galß-4Glcß-Cer | NeuAcα-3	<1
229	GalNAc-GD1a(Ac,Gc)	GalNAcß-4Galß-3GalNAcß-4Galß-4Glcß-Cer | | NeuGcα-3 NeuAcα-3 and/or GalNAcß-4Galß-3GalNAcß-4Galß-4Glcß-Cer | | NeuAcα-3 NeuGcα-3	<1
230	GD1b	Galß-3GalNAcß-4Galß-4Glcß-Cer | NeuAcα-8NeuAcα-3	<1
231	GD2	GalNAcß-4Galß-4Glcß-Cer | NeuAcα-8NeuAcα-3	<1
232	GT1a	NeuAcα-8NeuAcα-3Galβ-3GalNAcβ-4Galβ-4Glcβ-Cer | NeuAcα-3	<1
233	GT1b	NeuAcα-3Galβ-3GalNAcβ-4Galβ-4Glcβ-Cer | NeuAcα-8NeuAcα-3	<1
234	GQ1b	NeuAcα-8NeuAcα-3Galβ-3GalNAcβ-4Galβ-4Glcβ-Cer | NeuAcα-8NeuAcα-3	<1
235	SM1a	Galß-3GalNAcß-4Galß-4Glc-DH | SU-3	<1
236	SB2	SU-3GalNAcß-4Galß-4Glc-DH | SU-3	<1
237	SB1a	SU-3Galß-3GalNAcß-4Galß-4Glc-DH | SU-3	<1
238	GD1a-hexa	NeuAcα-3Galß-3GalNAcß-4Galß-4Glc-DH | NeuAcα-3	<1
239	GM1b	NeuAcα-3Galβ-3GalNAcß-4Galß-4Glcß-Cer***	9
240	SM2	GalNAcß-4Galß-4Glcß-Cer | SU-3	10
241	A8/1	GlcNAcα-4Galβ-OX	<1

242	A15/3	GlcNAcα-4Galβ-3Galβ-OX Fucα-2	<1
243	B13/b	GalNAcβ-4Galβ-3GlcNAcβ-OX KDNα-3	3
244	DSL	NeuAcα-3Galß-3GalNAc-DH NeuAcα-6	<1
245	A15/1	SU-6GlcNAcß-OY	<1
246	A8/2	SU-6 Fucα-3GlcNAcß-OY	3
247	B13/a-AO	GlcAβ-3Galβ-3GlcNAcβ-OX-AO	18
248	Notch-1	Fucα-Thr-DH	<1
249	Notch-2	GlcNAcβ-3Fucα-Thr-DH	<1
250	Notch-3	Galβ-3GlcNAcβ-3Fucα-Thr-DH	10
251	B12/3	GalNAcβ-4Galβ-OX NeuGcα-3	70
252	Man-Ser	Manα-Ser-DH	15
253	Man-Thr	Manα-Thr-DH	4
254	GalNAc-Thr	GalNAcα-Thr-DH	<1
255	GalNAc-Ser	GalNAcα-Ser-DH	7
256	Man-Thr-Succ	Manα-Thr-Succ-DH	<1
257	Man-Ser-Succ	Manα-Ser-Succ-DH	8
258	CSA-4	ΔUA-3GalNAcß-4GlcAß-3GalNAc-DH*** SU-4 SU-4	7
259	CSA-14	ΔUA-3GalNAcß-4GlcAß-3GalNAcß-4GlcAß-3GalNAcß-4GlcAß-3GalNAcß-4GlcAß-3GalNAcß-4GlcAß- SU-4 SU-4 SU-4 SU-4 SU-4 3GalNAcß-4GlcAß-3GalNAc-DH*** SU-4 SU-4	6
260	CSB-4	ΔUA-3GalNAcß-4IdoAα-3GalNAc-DH*** SU-4 SU-4	<1
261	CSB-14	ΔUA-3GalNAcß-4IdoAα-3GalNAcß-4IdoAα-3GalNAcß-4IdoAα-3GalNAcß-4IdoAα-3GalNAcß-4IdoAα- SU-4 SU-4 SU-4 SU-4 SU-4 3GalNAcß-4IdoAα-3GalNAc-DH*** SU-4 SU-4	14
262	CSC-4	ΔUA-3GalNAcß-4GlcAß-3GalNAc-DH*** SU-6 SU-6	5
263	CSC-14	ΔUA-3GalNAcß-4GlcAß-3GalNAcß-4GlcAß-3GalNAcß-4GlcAß-3GalNAcß-4GlcAß-3GalNAcß-4GlcAß- SU-6 SU-6 SU-6 SU-6 SU-6 3GalNAcß-4GlcAß-3GalNAc-DH*** SU-6 SU-6	<1
264	HA-4	GlcAß-3GlcNAcß-4GlcAß-3GlcNAc-DH	5
265	HA-14	GlcAß-3GlcNAcß-4GlcAß-3GlcNAcß-4GlcAß-3GlcNAcß-4GlcAß-3GlcNAcß-4GlcAß-3GlcNAcß-4GlcAß-3GlcNAcß-4GlcAß- 3GlcNAcß-4GlcAß-3GlcNAc-DH***	14
266	HEP-Di-IS	ΔUA-4GlcNS-DH*** SU-2 6-SU	12
267	HS-8	ΔUA-4GlcNAcα-4HexAß-4GlcNAcα-4HexAß-4GlcNAcα-4HexAß-4aMan-DH***	14
268	HEP-Di-IS-AO	ΔUA-4GlcNS-AO SU-2 6-SU	<1

	Homo-oligomers		
269	Glc2(α2)-AO	Glcα-2Glc-AO	<1
270	Glc2(α3)-AO	Glcα-3Glc-AO	555
271	Glc2(α4)-AO	Glcα-4Glc-AO	507
272	Glc3(α4)-AO	Glcα-4Glcα-4Glc-AO	30
273	Glc4(α4)-AO	Glcα-4Glcα-4Glcα-4Glc-AO	95
274	Malto-5-AO	Glcα-4Glcα-4Glcα-4Glcα-4Glc-AO	28
275	Malto-6-AO	Glcα-4Glcα-4Glcα-4Glcα-4Glcα-4Glc-AO	140
276	Malto-7-AO	Glcα-4Glcα-4Glcα-4Glcα-4Glcα-4Glcα-4Glc-AO	492
277	Glc2(α6)-AO	Glcα-6Glc-AO	42
278	Glc3(α6)-AO	Glcα-6Glcα-6Glc-AO	34
279	Glc4(α6)-AO	Glcα-6Glcα-6Glcα-6Glc-AO***	933
280	Glc5(α6)-AO	Glcα-6Glcα-6Glcα-6Glcα-6Glc-AO***	3805
281	Glc6(α6)-AO	Glcα-6Glcα-6Glcα-6Glcα-6Glcα-6Glc-AO***	5793
282	Glc7(α6)-AO	Glcα-6Glcα-6Glcα-6Glcα-6Glcα-6Glcα-6Glc-AO***	458
283	Glc2(ß3)-AO	Glcß-3Glc-AO	<1
284	Lam-3-AO	Glcß-3Glcß-3Glc-AO	<1
285	Lam-4-AO	Glcß-3Glcß-3Glcß-3Glc-AO	36
286	Lam-5-AO	Glcß-3Glcß-3Glcß-3Glcß-3Glc-AO	54
287	Lam-6-AO	Glcß-3Glcß-3Glcß-3Glcß-3Glcß-3Glc-AO***	285
288	Lam-7-AO	Glcß-3Glcß-3Glcß-3Glcß-3Glcß-3Glcß-3Glc-AO***	210
289	Glc2(ß4)-AO	Glcß-4Glc-AO	<1
290	Cello-3-AO	Glcß-4Glcß-4Glc-AO	<1
291	Cello-4-AO	Glcß-4Glcß-4Glcß-4Glc-AO	<1
292	Cello-5-AO	Glcß-4Glcß-4Glcß-4Glcß-4Glc-AO	38
293	Cello-6-AO	Glcß-4Glcß-4Glcß-4Glcß-4Glcß-4Glc-AO	22
294	Glc2(ß6)-AO	Glcß-6Glc-AO	<1
295	Pust-3-AO	Glcß-6Glcß-6Glc-AO	27
296	Pust-4-AO	Glcß-6Glcß-6Glcß-6Glc-AO***	<1
297	Pust-5-AO	Glcß-6Glcß-6Glcß-6Glcß-6Glc***	48
298	Pust-6-AO	Glcß-6Glcß-6Glcß-6Glcß-6Glcß-6Glc-AO***	238
299	Pust-7-AO	Glcß-6Glcß-6Glcß-6Glcß-6Glcß-6Glcß-6Glc-AO***	244
300	GalNAcα-3GalNAc	GalNAcα-3GalNAc-DH	<1
301	GN2	GlcNAcß-4GlcNAc-DH	<1
302	GN3	GlcNAcß-4GlcNAcß-4GlcNAc-DH	13
303	Man2(α6)	Manα-6Man-DH	22
304	Man5(ß4)	Manß-4Manß-4Manß-4Manß-4Man-DH	16
305	Man4(ß4)	Manß-4Manß-4Manß-4Man-DH	<1
306	Man6(ß4)	Manß-4Manß-4Manß-4Manß-4Manß-4Man-DH	20
307	Ara6(α5)	Araα-5Araα-5Araα-5Araα-5Araα-5Ara-DH	19
308	Ara7(α5)	Araα-5Araα-5Araα-5Araα-5Araα-5Araα-5Ara-DH	7
309	Xyl5(ß4)	Xylß-4Xylß-4Xylß-4Xylß-4Xyl-DH	13
	Miscellaneous		
310	Man3FXylGN2	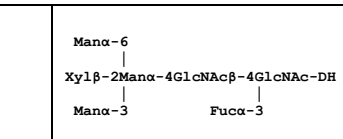	<1
311	Man3XylGN2	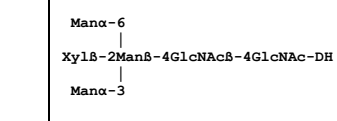	2
312	Galα-4Glc-AO	Galα-4Glc-AO	27

313	Xyl3Glc4	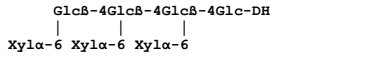	17
314	Gal4(α3,B4,α3)	Galα-3Galß-4Galα-3Gal-DH	<1
315	SU-Tyr	SU-Tyr-DH	8
316	Carra-Hexa-3S	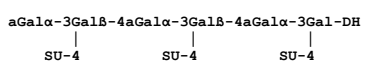	<1
317	Carra-Hexa-4S	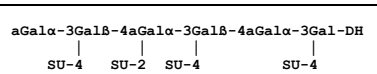	<1
318	Carra-Octa-4S	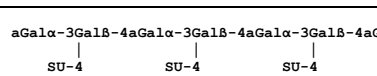	<1
319	Carra-Tetra-2S	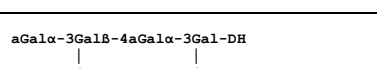	<1
320	Carra-Tetra-1S	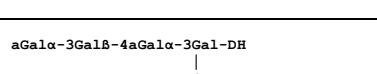	<1
321	Glc-AO	Glc-AO	13
322	GalNAc	GalNAc-DH	16
323	GalNAc-AO	GalNAc-AO	7
324	(6P)-Man	P-6Man-DH	13
325	(6P)-Man-AO	P-6Man-AO	15
326	Man	Man-DH	21
327	Man-AO	Man-AO	33
328	Fuc	Fuc-DH	15
329	Fuc-AO	Fuc-AO	62
330	Rha	Rha-DH	<1
331	Rha-AO	Rha-AO	11
332	GN	GlcNAc-DH	8
333	GN-AO	GlcNAc-AO	25
334	(6P)-Man5	P-6Manα-3Manα-3Manα-3Manα-2Man-DH	2
335	Glc4(α6,α4,α4)	Glcα-6Glcα-4Glcα-4Glc-DH	40

* The oligosaccharide probes are all lipid-linked, and are from the collection assembled in the course of research in Glycosciences Laboratory. DH, designates NGLs prepared from reducing oligosaccharides by reductive amination with the amino lipid, 1,2-dihexadecyl-*sn*-glycero-3-phosphoethanolamine (DHPE); OX and OY designate, respectively, the C1-4 fragment and the C5-6 fragments of GalNAcol of reduced oligosaccharides after mild periodate oxidation followed by reductive amination with DHPE (Chai et al., Methods Enzymol. 362, 160-195, 2003); AO, NGLs prepared from reducing oligosaccharides by oxime ligation with an aminooxy (AO) functionalized DHPE (Liu et al., Chem. Biol. 14, 847–859, 2007); Cer, natural glycolipids with various ceramide moieties; CerA and CerB denote different natural ceramides; Cer36 and Cer42, synthetic glycolipids with ceramide having a total of 36 and 42 carbon atoms, respectively; C30, a synthetic lipid [2-(tetradecyl)hexadecanol] with 30 carbon atoms. ΔUA, 4,5-unsaturated hexuronic acid; aMan, 2,5-anhydro-mannose; aGal, 3,6-anhydro-galactose.

** Pos, position in screening microarray.

*** Major component.